

A method for determining event-by-event elliptic flow fluctuations based on the first-order event plane in heavy-ion collisions

Gang Wang,¹ Declan Keane,² Aihong Tang,³ and Sergei A. Voloshin⁴

¹University of California, Los Angeles, California 90095

²Kent State University, Kent, Ohio 44242

³Brookhaven National Laboratory, Upton, New York 11973

⁴Wayne State University, Detroit, Michigan 48201

A new method is presented for determining event-by-event fluctuations of elliptic flow (v_2) using 1st-order event planes. By studying the event-by-event distributions of v_2 observables and 1st-order event-plane observables, average flow $\langle v_2 \rangle$ and event-by-event fluctuations with respect to that average can be separately determined, making appropriate allowance for the effects of finite multiplicity. The relation of flow fluctuations to eccentricity fluctuations in the initial-state participant region, as well as detector acceptance effects, are discussed. The method has been tested with Monte Carlo simulations.

PACS numbers: 25.75.Ld

In heavy-ion collisions, the azimuthal distributions of emitted particles can be decomposed with a Fourier expansion [1],

$$\frac{dN}{d\phi} = \frac{1}{2} f_0 + \sum_{n=1}^{\infty} 2v_n \cos(n(\phi - \phi_{RP})); \quad (1)$$

where ϕ and ϕ_{RP} denote the azimuthal angle of the particle and of the reaction plane, respectively. The Fourier coefficients,

$$v_n = \langle \cos(n(\phi - \phi_{RP})) \rangle; \quad (2)$$

are referred to as anisotropic flow of the n^{th} harmonic. The second harmonic, elliptic flow, carries information on the early stage of heavy-ion collisions, and has been extensively studied. Event-by-event flow fluctuations [2, 3, 4, 5] are of considerable interest because any fluctuation observable has potential relevance for phase transition phenomena, and because typical anisotropic flow measurements are dominated by systematic uncertainties in which flow fluctuations play a crucial role. At fixed centrality, initial-state fluctuations in the spatial anisotropy of the participant zone will cause flow fluctuations. In addition to this inevitable source of fluctuations, there might be additional fluctuation contributions that could offer unique insights into dynamical details of the collision process at very early times (1 fm/c and earlier). The large observed elliptic flow at RHIC points to very short thermal equilibration time in the framework of hydrodynamic models. This puzzling feature calls for further investigation and could have alternative explanations or might be explained by exotic phenomena [6, 7, 8, 9].

RHIC data hold much promise for the purpose of understanding elliptic flow fluctuations, since y is large,

while the statistical noise arising from finite multiplicity, that tends to obscure the dynamical fluctuations of interest, is smaller than at lower energies. Most flow analyses at RHIC to date have relied on the second-order event plane, whereas in the present study, a case is presented for utilizing the first-order event plane to determine the mean elliptic flow in any sample, and to isolate the sought-after dynamical fluctuations about that mean. In RHIC experiments, first-order event planes can be obtained, for example, via the ZDC-SMD (Shower Maximum Detector) [10] or the Forward TPC [11] of the STAR detector. In the scenario envisaged here, the fluctuating anisotropies are based on measurements near midrapidity, while the first-order event plane determination utilizes detectors that are far removed in rapidity. Consequently, non-flow effects (correlations that may contribute to v_n but which are unrelated to the event reaction plane) are believed to be negligible using this method [12]. With two independent 1st-order event planes a and b , elliptic flow can be determined with the help of the relations

$$\begin{aligned} v_2^{\text{obs}} &= \langle \cos(2(\phi_a - \phi_b)) \rangle \\ &= \langle \cos(2(\phi - \phi_{RP})) \rangle \langle \cos(2(\phi_{RP} - \phi_a - \phi_b)) \rangle \\ &= v_2 \langle \cos(\phi_a - \phi_b) \rangle; \end{aligned} \quad (3)$$

where the last factor, $\langle \cos(\phi_a - \phi_b) \rangle$ is usually called the reaction plane resolution [1]. The above is based on the assumptions that the two first-order reaction planes are independent, and that the distributions of a and b with respect to the true reaction plane are symmetric.

We introduce two event-by-event quantities, $C_2^{\text{obs};k}$ and $S_2^{\text{obs};k}$, where index k denotes the k^{th} event. Using the equality

$$\begin{aligned} \cos(2' \quad a_{jk} \quad b_{jk}) &= \cos[2' \quad (a_{jk} \quad b_{jk})] \\ &= \cos 2' \quad (a_{jk} \quad b_{jk}) + \sin 2' \quad (a_{jk} \quad b_{jk}); \end{aligned} \quad (4)$$

where $a_{jk} = a_{jk} \quad R P$ and $b_{jk} = b_{jk} \quad R P$, and averaging over all particles in a single event, we define

$$c_2^{obs;jk} = c_2^{(k)} \cos(a_{jk} + b_{jk}) + s_2^{(k)} \sin(a_{jk} + b_{jk}) \quad (5)$$

$$s_2^{obs;jk} = s_2^{(k)} \cos(a_{jk} + b_{jk}) - c_2^{(k)} \sin(a_{jk} + b_{jk}) \quad (6)$$

Note that, averaged over all events, $hc_2^{obs;jk} i = v_2^{obs}$, $hs_2^{obs;jk} i = 0$, $hc_2^{(k)} i = v_2$, and $hs_2^{(k)} i = 0$.

Each quantity in Eq. (5) is an instance (or element) of its own distribution (or set) [13]. Thus the distribution of $c_2^{obs;jk}$ is related to the distributions of $c_2^{(k)}$, $s_2^{(k)}$, and $(a_{jk} + b_{jk})$ according to

$$\begin{aligned} fc_2^{obs;jk} g &= fc_2^{(k)} g \quad f\cos(a_{jk} + b_{jk}) g \\ &\quad fs_2^{(k)} g \quad f\sin(a_{jk} + b_{jk}) g \end{aligned} \quad (7)$$

where the operators f and g demonstrate the relationship between the instances of the distributions, instead of between the distributions themselves [13]. Here we assume that the distribution of the first-order event planes $f_{a_{jk} + b_{jk}} g$ is independent of $fc_2^{(k)} g$ and $fs_2^{(k)} g$. This assumption is usually not valid for second-order event planes, and this illustrates one of the advantages of the present approach. We further assume that $f_{a_{jk}} g$ and $f_{b_{jk}} g$ are both symmetric around zero, so that $f_{a_{jk} + b_{jk}} g$ and $f_{a_{jk} - b_{jk}} g$ are identical. Thus Eq. (7) becomes

$$\begin{aligned} fc_2^{obs;jk} g &= fc_2^{(k)} g \quad f\cos_{ab;jk} g \\ &\quad fs_2^{(k)} g \quad f\sin_{ab;jk} g; \end{aligned} \quad (8)$$

where $ab;jk = a_{jk} - b_{jk} = a_{jk} + b_{jk}$. Note that the cosine part and the sine part on the r.h.s. of Eq. (8) are not independent. However, in the procedure for estimating the mean and RMS values of v_2 (all that is required in the present analysis), the cross term vanishes due to symmetry, so we can treat these two parts as independent. In a similar way, the distribution $fs_2^{obs;jk} g$ becomes

$$\begin{aligned} fs_2^{obs;jk} g &= fs_2^{(k)} g \quad f\cos_{ab;jk} g \\ &\quad fc_2^{(k)} g \quad f\sin_{ab;jk} g; \end{aligned} \quad (9)$$

In the following discussion, we use the same convention as in Ref. [13], where $E f x g$ and $f x g$ denote the mean (or expectation value) and the RMS (or standard deviation), respectively, of the distribution $f x g$. The distribution relations, Eqs. (8) and (9) can be rewritten in terms of mean values:

$$\begin{aligned} E fc_2^{obs;jk} g &= E fc_2^{(k)} g E f\cos_{ab;jk} g \\ &\quad + E fs_2^{(k)} g E f\sin_{ab;jk} g \end{aligned} \quad (10)$$

$$\begin{aligned} E fs_2^{obs;jk} g &= E fs_2^{(k)} g E f\cos_{ab;jk} g \\ &\quad - E fc_2^{(k)} g E f\sin_{ab;jk} g; \end{aligned} \quad (11)$$

The latter equations can be resolved with respect to mean values of $fc_2^{(k)} g$ and $fs_2^{(k)} g$:

$$\begin{aligned} E fc_2^{(k)} g &= [E fc_2^{obs;jk} g E f\cos_{ab;jk} g \\ &\quad - E fs_2^{obs;jk} g E f\sin_{ab;jk} g] / \\ &\quad [E^2 f\cos_{ab;jk} g + E^2 f\sin_{ab;jk} g] \end{aligned} \quad (12)$$

$$\begin{aligned} E fs_2^{(k)} g &= [E fs_2^{obs;jk} g E f\cos_{ab;jk} g \\ &\quad + E fc_2^{obs;jk} g E f\sin_{ab;jk} g] / \\ &\quad [E^2 f\cos_{ab;jk} g + E^2 f\sin_{ab;jk} g]; \end{aligned} \quad (13)$$

Everything on the r.h.s. of Eq. (12) and (13) is an experimental observable. In the case $E f\sin_{ab;jk} g E f\cos_{ab;jk} g = 0$, Eq. (12) and (13) reduce to

$$E fc_2^{(k)} g = E fc_2^{obs;jk} g / E f\cos_{ab;jk} g \quad (14)$$

$$E fs_2^{(k)} g = E fs_2^{obs;jk} g / E f\cos_{ab;jk} g \quad (15)$$

Normally, $E f\cos_{ab;jk} g$ is regarded as a correction for the event plane resolution.

The RMS values of the v_2 distributions in Eq. (8) and (9) are calculable as per

$$\begin{aligned} {}^2 fc_2^{obs;jk} g &= E^2 fc_2^{(k)} g {}^2 f\cos_{ab;jk} g + {}^2 fc_2^{(k)} g E f\cos_{ab;jk} g \\ &\quad + E^2 fs_2^{(k)} g {}^2 f\sin_{ab;jk} g + {}^2 fs_2^{(k)} g E f\sin_{ab;jk} g \end{aligned} \quad (16)$$

$$\begin{aligned} {}^2 fs_2^{obs;jk} g &= E^2 fc_2^{(k)} g {}^2 f\sin_{ab;jk} g + {}^2 fc_2^{(k)} g E f\sin_{ab;jk} g \\ &\quad + E^2 fs_2^{(k)} g {}^2 f\cos_{ab;jk} g + {}^2 fs_2^{(k)} g E f\cos_{ab;jk} g \end{aligned} \quad (17)$$

We can solve Eqs. (16) and (17) for $f_{C_2}^{(k)}g$ and $f_{S_2}^{(k)}g$,

$$f_{C_2}^{(k)}g = \frac{V E f \cos^2_{ab;k}g - S E f \sin^2_{ab;k}g}{E^2 f \cos^2_{ab;k}g - E^2 f \sin^2_{ab;k}g} \quad (18)$$

$$f_{S_2}^{(k)}g = \frac{S E f \cos^2_{ab;k}g - V E f \sin^2_{ab;k}g}{E^2 f \cos^2_{ab;k}g - E^2 f \sin^2_{ab;k}g} \quad (19)$$

where

$$V = f_{C_2}^{obs;k}g - E^2 f_{C_2}^{(k)}g - f_{S_2}^{(k)}g \quad (20)$$

$$S = f_{S_2}^{obs;k}g - E^2 f_{C_2}^{(k)}g - f_{S_2}^{(k)}g \quad (21)$$

Eqs. (18) and (19) are valid and useful only when $E f \cos^2_{ab;k}g$ and $E f \sin^2_{ab;k}g$ are significantly different from each other. According to Eqs. (1)–(2), we know that

$$\hbar \cos^2 n(\theta_r) = 0.5(1 + v_{2n}) \quad (22)$$

$$\hbar \sin^2 n(\theta_r) = 0.5(1 - v_{2n}) \quad (23)$$

When we expand the distributions $f_{a;k}g$ and $f_{b;k}g$ in the same way as in Eq. (1), we have the $n = 1$ case

$$E f \cos^2_{ab;k}g = 0.5(1 + v_{2a}v_{2b}) \quad (24)$$

$$E f \sin^2_{ab;k}g = 0.5(1 - v_{2a}v_{2b}) \quad (25)$$

where v_{2a} and v_{2b} are v_2 in the rapidity regions where the first-order event planes are determined. If v_{2a} and v_{2b} are very small compared with 1, $E f \cos^2_{ab;k}g$ and $E f \sin^2_{ab;k}g$ will be close to each other, and Eqs. (18) and (19) no longer hold. In this case, Eqs. (16) and (17) are not independent. Eq. (16) transforms into

$$f_{C_2}^{(k)}g + f_{S_2}^{(k)}g = 2V \quad (26)$$

The observed fluctuations $f_{C_2}^{(k)}g$ and $f_{S_2}^{(k)}g$ each have two contributions: dynamical and statistical fluctuations.

$$f_{C_2}^{(k)}g = f_{dyn}^{(k)}g + f_{stat}^{(k)}g \quad (27)$$

$$= f_{dyn}^{(k)}g + 0.5(1 + v_4 - 2E^2 f_{C_2}^{(k)}g)M$$

$$f_{S_2}^{(k)}g = f_{dyn}^{(k)}g + f_{stat}^{(k)}g \quad (28)$$

$$= f_{dyn}^{(k)}g + 0.5(1 - v_4 - 2E^2 f_{S_2}^{(k)}g)M;$$

where M denotes multiplicity, and the v_4 term arises from setting $n = 2$ in Eqs. (22) and (23). v_4 is usually negligible compared with 1. Now Eq. (26) becomes

$$2V = (1 - E^2 f_{C_2}^{(k)}g - E^2 f_{S_2}^{(k)}g)M \quad (29)$$

In the case where the distribution $f_{RP}g$ is symmetric around zero, $E f_{S_2}^{(k)}g$ and $f_{dyn}^{(k)}g$ vanish, and Eq. (29) reduces to

$$f_{C_2}^{(k)}g = 2V = (1 - E^2 f_{C_2}^{(k)}g)M \quad (30)$$

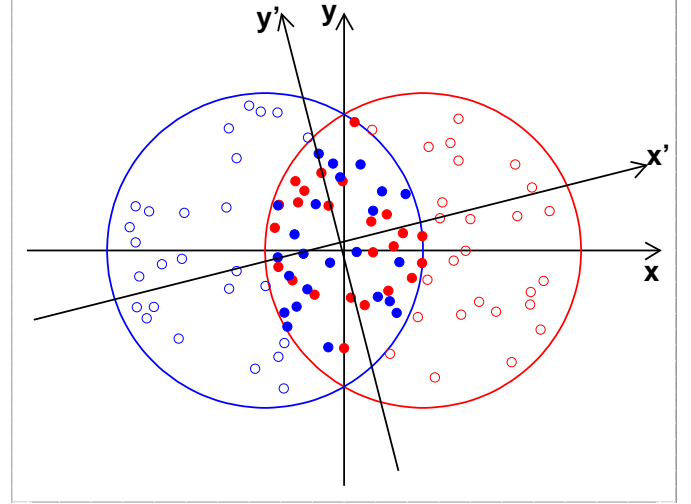


FIG. 1: (color online) Schematic representation, in the plane transverse to the beam (z) direction, of a collision between two identical nuclei. The x - and y -axes are drawn as per the standard convention. The solid circles illustrate a possible configuration of the participant nucleons. Due to the fluctuation of this event, the overlap zone is shifted and tilted with respect to the $(x; y)$ frame. x^0 and y^0 are the principal axes of inertia of the solid circles.

In heavy-ion collisions, due to the finite number of participants, the overlap zone could be translated and rotated with respect to the conventional coordinate system, as illustrated in Fig. 1. As a result, the final produced particles are symmetrically distributed about the x^0 axis, instead of the x axis. In this paper, we neglect the translation, and only consider the rotation of the overlap zone. We define the angle between x^0 and x direction to be θ_k for the k^{th} event, and $f_{C_2}^{(k)}$ becomes

$$f_{C_2}^{(k)} = \hbar \cos 2(\theta_{RP} + \theta_k) = f_{C_2}^{0(k)} \cos 2\theta_k + f_{S_2}^{0(k)} \sin 2\theta_k; \quad (31)$$

where $f_{C_2}^{0(k)}$ and $f_{S_2}^{0(k)}$ are measured along the x^0 axis. In the same way, $f_{S_2}^{(k)}$ becomes

$$f_{S_2}^{(k)} = f_{C_2}^{0(k)} \sin 2\theta_k + f_{S_2}^{0(k)} \cos 2\theta_k; \quad (32)$$

The mean values of $f_{c_2}^{(k)}g$ and $f_{s_2}^{(k)}g$ are related to those of $f_{c_2}^{0(k)}g$ by

$$E f_{c_2}^{(k)}g = E f_{c_2}^{0(k)}g E f \cos 2'_{\alpha, \beta} g \quad (33)$$

$$E f_{s_2}^{(k)}g = E f_{c_2}^{0(k)}g E f \sin 2'_{\alpha, \beta} g \quad (34)$$

$E f_{s_2}^{0(k)}g$ goes to zero, due to symmetry. Therefore $E f_{c_2}^{(k)}g$ is always less than or equal to $E f_{c_2}^{0(k)}g$. If the distribution $f_{\alpha, \beta} g$ is symmetric around zero, then $E f_{s_2}^{(k)}g$ vanishes. $f_{\alpha, \beta} g$ can be simulated, for example, in a Glauber calculation [14].

Eqs. (31) and (32) give another useful relationship,

$$(c_2^{(k)})^2 + (s_2^{(k)})^2 = (c_2^{0(k)})^2 + (s_2^{0(k)})^2 \quad (35)$$

Since we focus on dynamical fluctuations, we take the limit $M \rightarrow 1$ when examining Eq. (35) from event to event. Then the distribution $f_{c_2}^{0(k)}g$ is subject to the constraint

$$E^2 f_{c_2}^{0(k)}g + \langle \frac{2}{d_{\text{dyn}}} f_{c_2}^{0(k)}g \rangle = E^2 f_{c_2}^{(k)}g + \langle \frac{2}{d_{\text{dyn}}} f_{c_2}^{(k)}g \rangle + E^2 f_{s_2}^{(k)}g + \langle \frac{2}{d_{\text{dyn}}} f_{s_2}^{(k)}g \rangle \quad (36)$$

The measurement of the quantities on the r.h.s. of Eq. (36) has been discussed, and their sum provides a way to estimate the upper limit for $E f_{c_2}^{0(k)}g$, which corresponds to the lower limit for $E f \cos 2'_{\alpha, \beta} g$. Once $f_{\alpha, \beta} g$ is simulated, we are able to measure the elliptic flow and its dynamical fluctuation, not only along the x axis, but also along x^0 .

Another way to measure v_2 fluctuations along the x^0 axis is through eccentricity. The standard definition of eccentricity for the k^{th} event is

$$e_k = \frac{h y_k^2 - x_k^2 i}{h y_k^2 + x_k^2 i} \quad (37)$$

where x_k and y_k denote the participant coordinates. The coordinates $(x; y)$ and $(x^0; y^0)$ are linked by the rotation through α, β ,

$$\begin{aligned} x_k &= x_k^0 \cos \alpha - y_k^0 \sin \alpha \\ y_k &= x_k^0 \sin \alpha + y_k^0 \cos \alpha \end{aligned} \quad (38)$$

Then

$$\begin{aligned} y_k^2 + x_k^2 &= (y_k^0)^2 + (x_k^0)^2 \\ \frac{y_k^2 - x_k^2}{y_k^2 + x_k^2} &= \left[\frac{(y_k^0)^2 - (x_k^0)^2}{(y_k^0)^2 + (x_k^0)^2} \right] \cos 2'_{\alpha, \beta} \\ &\quad + 2 \frac{x_k^0 y_k^0}{(y_k^0)^2 + (x_k^0)^2} \sin 2'_{\alpha, \beta} \end{aligned} \quad (39)$$

Thus the eccentricities in the two coordinate systems are related according to

$$e_k = e_k^0 \cos 2'_{\alpha, \beta} + \frac{2 x_k^0 y_k^0 \sin 2'_{\alpha, \beta}}{(y_k^0)^2 + (x_k^0)^2} \quad (40)$$

The mean values of $f_{\alpha, \beta} g$ and $f_{\alpha, \beta}^0 g$ have the same relationship as $f_{c_2}^{(k)}g$ and $f_{c_2}^{0(k)}g$ in Eq. (33), i.e.,

$$E f_{\alpha, \beta} g = E f_{\alpha, \beta}^0 g E f \cos 2'_{\alpha, \beta} g \quad (41)$$

As long as the ratio between $E f_{\alpha, \beta} g$ and $E f_{\alpha, \beta}^0 g$ is known, we can calculate v_2 and its fluctuation along the x^0 axis.

To allow for detector imperfections, we can break down the v_2 observable into cosine and sine components.

$$v_{2 \cos}^{\text{obs}} = h 2 \cos 2'_{\alpha, \beta} \cos(\alpha + \beta) i \quad (42)$$

$$v_{2 \sin}^{\text{obs}} = h 2 \sin 2'_{\alpha, \beta} \sin(\alpha + \beta) i \quad (43)$$

In the k^{th} event, we have

$$\begin{aligned} c_{2 \cos}^{\text{obs}; k} &= c_2^{\text{obs}; k} + h \cos(2'_{\alpha, \beta} + \alpha_{jk} + \beta_{jk}) i \\ &= 2 h \cos^2 2'_{\alpha, \beta} i c_2^{\text{obs}; k} + h \sin 4'_{\alpha, \beta} i s_2^{\text{obs}; k} \end{aligned} \quad (44)$$

$$\begin{aligned} c_{2 \sin}^{\text{obs}; k} &= c_2^{\text{obs}; k} h \cos(2'_{\alpha, \beta} + \alpha_{jk} + \beta_{jk}) i \\ &= 2 h \sin^2 2'_{\alpha, \beta} i c_2^{\text{obs}; k} - h \sin 4'_{\alpha, \beta} i s_2^{\text{obs}; k} \end{aligned} \quad (45)$$

If α, β can be measured with negligible detector imperfections, then $h \sin 4'_{\alpha, \beta} i$ should vanish, and there is no difference between $h \cos^2 2'_{\alpha, \beta} i$ and $h \sin^2 2'_{\alpha, \beta} i$. Otherwise, $E f_{c_{2 \cos}^{\text{obs}; k}} g$ and $E f_{c_{2 \sin}^{\text{obs}; k}} g$ will be different from each other, and from $E f_{c_2^{\text{obs}; k}} g$. In some of the cases previously mentioned, $E f_{s_2^{\text{obs}; k}} g$ goes to zero, and we may consider $h \cos^2 2'_{\alpha, \beta} i$ and $h \sin^2 2'_{\alpha, \beta} i$ to be correction factors for the detector deficiencies.

We can further separate the v_2 observable into four terms:

$$v_{2 \cos^0}^{\text{obs}} = h 4 \cos 2'_{\alpha, \beta} \cos \alpha \cos \beta i \quad (46)$$

$$v_{2 \cos^{00}}^{\text{obs}} = h 4 \cos 2'_{\alpha, \beta} \sin \alpha \sin \beta i \quad (47)$$

$$v_{2 \sin^0}^{\text{obs}} = h 4 \sin 2'_{\alpha, \beta} \sin \alpha \cos \beta i \quad (48)$$

$$v_{2 \sin^{00}}^{\text{obs}} = h 4 \sin 2'_{\alpha, \beta} \cos \alpha \sin \beta i \quad (49)$$

By way of example, we next consider the first term in the k^{th} event.

$$\begin{aligned} c_{2 \cos^0}^{\text{obs}; k} &= [1 + h \cos 4'_{\alpha, \beta} i + \cos 2'_{\alpha, \beta} \cos 2'_{\beta, \beta} i] c_2^{\text{obs}; k} \\ &\quad + [h \sin 4'_{\alpha, \beta} i \sin 2'_{\alpha, \beta} \sin 2'_{\beta, \beta} i] s_2^{\text{obs}; k} \end{aligned} \quad (50)$$

If α, β and α, β are all measured with negligible detector imperfections, then $E f_{c_{2 \cos^0}^{\text{obs}; k}} g = E f_{c_2^{\text{obs}; k}} g$. When $h \cos 4'_{\alpha, \beta} i$, $h \cos 2'_{\alpha, \beta} \cos 2'_{\beta, \beta} i$ and $h \cos 2'_{\beta, \beta} \cos 2'_{\alpha, \beta} i$ are all very small compared with 1, the correction factor can be approximated according to

$$\begin{aligned} &1 + h \cos 4'_{\alpha, \beta} i + \cos 2'_{\alpha, \beta} \cos 2'_{\beta, \beta} i \\ &[1 + h \cos 4'_{\alpha, \beta} i] [1 + h \cos 2'_{\alpha, \beta} i] [1 + h \cos 2'_{\beta, \beta} i] \\ &= 2 h \cos^2 2'_{\alpha, \beta} i 2 h \cos^2 2'_{\alpha, \beta} i 2 h \cos^2 2'_{\beta, \beta} i \end{aligned} \quad (51)$$

The other three terms of the v_2 observable can be treated in a similar way.

The methods described above have been tested in a Monte Carlo simulation. In the first set of simulations, the input particles in each event carry 5% mean elliptic flow and 3% dynamical fluctuation. For the first-order event planes, we set $v_{1a} = v_{1b} = 20\%$, which corresponds to $h \cos 2'_{\alpha, \beta} i = 4\%$. Five multiplicities are

Multiplicity	$E \langle v_2^{(k)} \rangle g$ (%)	$_{\text{dyn}} \langle v_2^{(k)} \rangle g$ (%)
25	4:90 0:12	3:16 0:18
50	4:97 0:09	3:00 0:14
100	4:90 0:07	3:14 0:11
200	4:96 0:06	3:03 0:10
400	5:05 0:05	2:94 0:09

TABLE I: Results for the extracted mean v_2 for an input of 5%, and its dynamical fluctuation for an input of 3%, based on simulated events with different multiplicities. The errors are statistical.

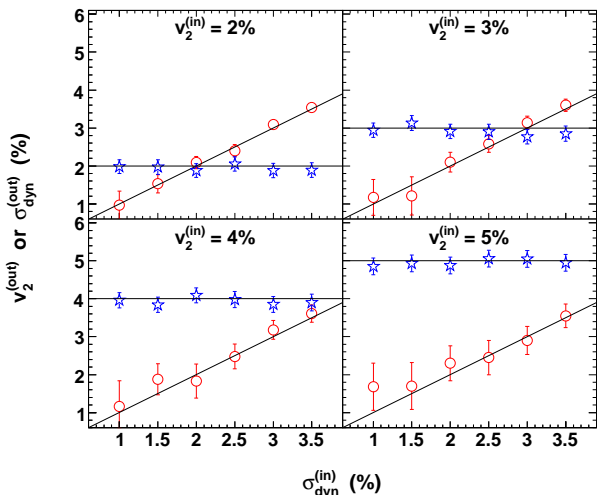


FIG. 2: (color online) The reconstructed mean v_2 (stars) and its dynamical fluctuation (circles) as functions of input $_{\text{dyn}} \langle v_2^{(k)} \rangle g$ for Monte Carlo events with multiplicity of 100. Panels are shown for input $E \langle v_2^{(k)} \rangle g$ ranging from 2% to 5%. The errors are statistical.

tested: $M = 25, 50, 100, 200$ and 400 . In each case, ten million events were generated. Table I lists the output

results. Over a broad range of multiplicities, the output results agree with the input values, well within the statistical errors of the simulation.

We have also explored the robustness of the method with variations in the input values of $E \langle v_2^{(k)} \rangle g$ and $_{\text{dyn}} \langle v_2^{(k)} \rangle g$. In this second group of tests, the multiplicity was fixed at $M = 100$, and one million events were generated in each case. The reconstructed mean v_2 and the extracted dynamical fluctuation values are shown in Fig. 2.

In summary, various suggestions in the literature point to dynamical event-by-event fluctuations in elliptic flow as being of great interest in the realm of RHIC physics, and such fluctuations are argued to be especially relevant for understanding collision dynamics at the earliest times. On a more technical level in experimental methodology, the magnitude of flow fluctuations associated with current elliptic flow measurement is not understood, and this uncertainty affects the overall systematic error on these measurements. Prompted by the above considerations, this work presents a new method for experimental analysis of elliptic flow in a scenario where the first-order event plane can be resolved. The method allows the extraction of mean v_2 and its dynamical event-by-event fluctuations, and good immunity to both statistical fluctuations and non-flow effects can be expected. Fluctuations in spatial eccentricity in the initial-state participant region have been considered, as have detector acceptance effects. Simulations have been presented that validate the method under a range of conditions similar to those observed in RHIC data.

Acknowledgments

We acknowledge useful discussions with Art Poskanzer, Rainald Snellings, Paul Sorensen, and we thank them for their helpful suggestions.

-
- [1] S. Voloshin and Y. Zhang, Z. Phys. C 70, 665 (1996); A. M. Poskanzer and S. A. Voloshin, Phys. Rev. C 58, 1671 (1998).
- [2] STAR Collaboration, C. Adler et al., Phys. Rev. C 66, 034904 (2002).
- [3] STAR Collaboration, J. Adams et al., Phys. Rev. C 72, 014904 (2005).
- [4] M. Miller and R. Snellings, preprint nucl-ex/0312008
- [5] PHOBOS collaboration, B. Alver et al., preprint nucl-ex/0608025
- [6] S. Mrowczynski, Phys. Lett. B 314, 118 (1993); Phys. Rev. C 49, 2191 (1994); Phys. Lett. B 393, 26 (1997).
- [7] Y. V. Kovchegov and K. L. Tuchin, Nucl. Phys. A 708, 413 (2002).
- [8] A. Karsnitz, Y. Nara and R. Venugopalan, Phys. Lett. B 554, 21 (2003).
- [9] E. Shuryak, Nucl. Phys. A 715, 289 (2003).
- [10] C. Adler et al., Nucl. Instr. Meth. A 470, 488 (2001); The STAR ZDC-SMD has the same structure as the STAR EEMC SMD: C. E. Alger et al., Nucl. Instr. Meth. A 499, 740 (2003); STAR ZDC-SMD proposal, STAR Note SN-0448 (2003).
- [11] K. H. Ackermann et al., Nucl. Instr. Meth. A 499, 713 (2003).
- [12] STAR Collaboration, J. Adams et al., Phys. Rev. C 73, 034903 (2006).
- [13] D. A. S. Fraser, Statistics: An Introduction (John Wiley, New York, 1960).
- [14] B. B. Back et al., Phys. Rev. C 65, 031901 (2002); K. Adcox et al., Phys. Rev. Lett. 86, 3500 (2001); I. G.

Bearden et al., Phys. Lett. B 523, 227 (2001); STAR
Collaboration, J. Adams et al., Phys. Rev. C 70, 054907 (2004).